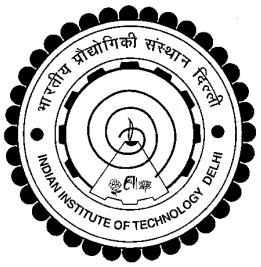

Dept of Physics, IIT Delhi

Course Code: PYD411
Academic Year: 2025 - 2026, Semester - I

Dependence of Phase Measurement Error on Object Sparsity

Shruti Aparna (2022PH11850)
Anushka Pandey (2022PH11848)

Adviser: Prof. Kedar Khare
Co-Advisor: Prof. Pradipta Ghosh

Abstract: Accurate phase measurement is crucial for applications such as gravitational-wave detection and biomedical imaging. As a result of the shot-noise limit, the measurement precision of classical interferometric systems scales as $\sqrt{N}$. Quantum resources, including squeezed light, can exceed this limit in single-point measurements; however, they do not scale effectively for multi-pixel imaging. This study examines the potential of utilising spatial redundancy and correlations among adjacent pixels to enhance phase estimation with classical light alone. We create algorithms for reconstruction driven by sparsity and establish a phase-only optimisation framework that maintains the amplitude of the object. We evaluate our methods using real data obtained from transparent red blood cell samples through a digital holographic microscope, illustrating their practical effectiveness for high-precision multipixel phase retrieval.

Signature of student: ..... **Signature of the adviser:** .....

Signature of student: .....

1 Introduction

1.1 Background and motivation

Interferometric phase measurement is essential for various scientific and technical applications, such as gravitational-wave detection in LIGO, high-resolution optical metrology, and developing quantum sensing platforms. In all such systems, the capacity to precisely determine the phase difference between optical fields directly influences the sensitivity and efficacy of the measurement. Conventional interferometric techniques are naturally restricted by photon shot noise arising from the quantum properties of light. The shot-noise limit (SNL) restricts the achievable phase precision to a scale of $1/\sqrt{N}$, with N representing the number of observed photons. Furthermore, technical noise, ambient disturbances, and detector inefficiencies might impair measurement accuracy and make it more difficult to implement the SNL in practice. Although methods such as averaging and advancements in detector technology may assist in approaching the Standard Quantum Limit (SNL), they are insufficient for surpassing it. To improve phase sensitivity over the shot noise limit, quantum resources such as compressed states or entangled photons must be used. However, these technologies increase complexity and have yet to be widely integrated into mainstream measurement systems.

1.2 Traditional Phase Measurement Limitations

Conventional phase measurement techniques, such as phase-shifting methods (PSM), treat individual pixels or measurement points as independent entities. This single-pixel-based approach leads to several limitations, like the phase accuracy scales as $1/\sqrt{N}$, where N is the number of detected photons. This method also doesn't consider correlations between neighbouring pixels. Spatial redundancy and smoothness constraints are also ignored. Performance degrades rapidly in low-photon regimes.

1.3 Quantum Enhanced Approach

While quantum mechanical approaches using squeezed light and entangled states can surpass the classical SNL, they require specialised light sources and complex experimental setups. The fundamental question arises: Can we achieve better than $1/\sqrt{N}$ scaling using classical light by exploiting the inherent structure and sparsity of the phase object?

1.4 Research Objective

This study aims to:

1. Develop computational algorithms for enhanced phase estimation using classical light
2. Investigate the relationship between object sparsity or complexity and phase measurement accuracy
3. Evaluate constrained optimization methods for multipixel phase recovery

2 Theoretical Framework

2.1 Traditional Single-Pixel Phase Analysis

In a typical interferometric setup, when a signal of interest interferes with a reference beam, the detected photon counts at the two output ports of a balanced detector are

given by:

$$N_1 \approx (N/2)[1 + \sin(\Delta\phi)]$$
$$N_2 \approx (N/2)[1 - \sin(\Delta\phi)]$$
Signal of interest and noise (Poisson statistics)
$$N_s = N_1 - N_2 = N\sin(\Delta\phi)$$
$$\sigma_{N_s} = \sqrt{\sigma_{N_1}^2 + \sigma_{N_2}^2} = \sqrt{N}$$
$$\Delta\phi \sim 1/\sqrt{N} \text{ (standard quantum limit).}$$

The traditional analysis assumes that each pixel or measurement point is independent.

2.2 Interferometric Signal Model

When two complex fields, R (reference) and O (object), interfere, the detected intensity is given by:

$$I = |R|^2 + |O|^2 + R^*O + RO^* \tag{1}$$

The phase ϕ_O of the object field relative to the reference phase ϕ_R can be extracted using various methods. One such method is the Phase Shifting Method (PSM).

2.3 Phase Shifting Methods

The conventional four-frame phase-shifting method uses reference phase shifts $\theta = 0, \pi/2, \pi, 3\pi/2$:

$$\phi_O - \phi_R = \arctan[(I_{3\pi/2} - I_{\pi/2})/(I_0 - I_\pi)] \tag{2}$$

This method assumes independent pixels and achieves shot-noise-limited performance.

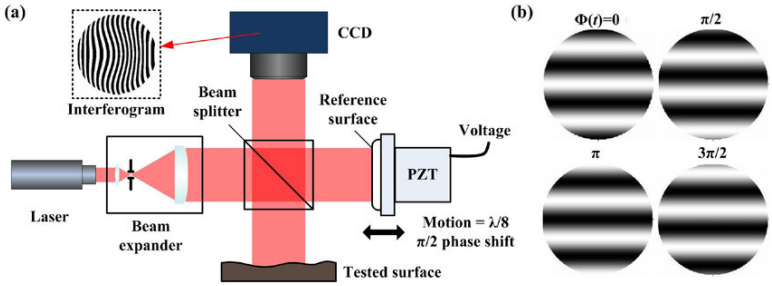

Figure 1: Schematic of a phase-shifting interferometer showing sequential frames acquired with controlled phase shifts introduced by a PZT actuator (Griesmann [6]).

2.4 Constrained Optimisation Framework

The optimisation approach minimises a cost function:

$$C(O, O^*) = ||\beta(I)[I - (|R|^2 + |O|^2 + R^*O + RO^*)]||^2 + \alpha\psi(O, O^*) \tag{3}$$

where

- First term: weighted L2-norm data fidelity
- Second term: regularisation constraint modelling object properties
- α: regularisation parameter balancing data fidelity and constraints

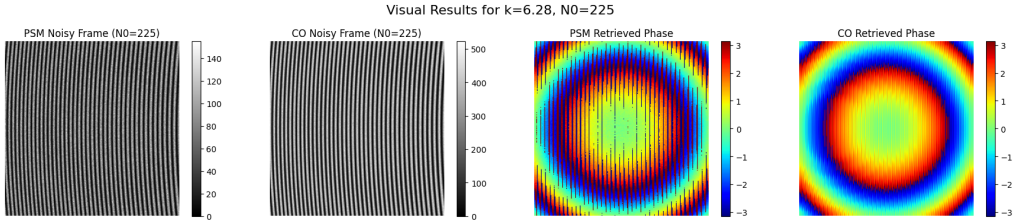

Figure 2: Comparison of phase shifting & optimisation algorithm which uses TV penalty function for photon count 225 & curvature of spherical wavefront k=6.28

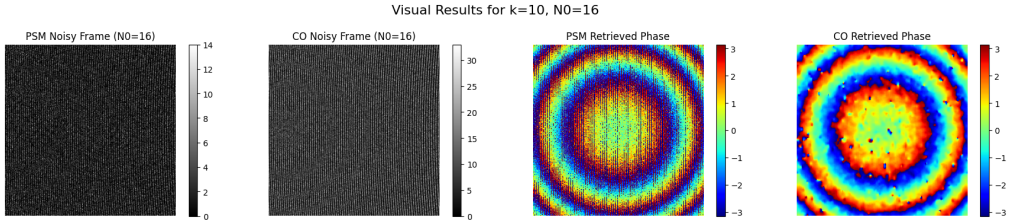

Figure 3: Comparison of phase shifting & optimisation algorithm which uses immediate 4-neighbourhood penalty function for photon count 16 & curvature of spherical wavefront k=10

2.4.1 TV optimisation

To enforce spatial smoothness in the reconstructed object field, we incorporate a Total Variation (TV)–based smoothness penalty. In our implementation, we use the quadratic (or "second-order") form of TV, defined over the complex field O(x,y) as:

$$\Psi_{\mathrm{TV}}(O) = \sum_{x,y} \left(|\nabla_x O(x,y)|^2 + |\nabla_y O(x,y)|^2 \right), \tag{4}$$

The effect of the TV penalty on the reconstruction quality can be visually observed in Fig. 2, where the TV-optimised phase retrieval produces smoother, less noisy phase estimates compared to the unregularised result.

2.4.2 Neighborhood Smoothness Penalty

To promote local smoothness in the reconstructed object field, we use a generalised neighbourhood-based L2 penalty of the form as described in Singh's work [1] in eq. 6:

$$\Psi_{\mathrm{nb}}(O) = \sum_{p} \sum_{q \in N_p} w_{pq} \, | \, O_p - O_q \, |^2, \tag{5}$$

where p indexes each pixel and q runs over a chosen neighbourhood N_p of pixel p. The weights w_{pq} control the contribution of each neighbor and may encode simple adjacency (4- or 8-neighbour) or a distance-based window (e.g., Gaussian). This penalty discourages large variations between a pixel and the values in its local neighbourhood, resulting in a smoother and more physically consistent reconstruction of the object field. The improvement introduced by neighbourhood regularisation is illustrated in Fig. 3 and Fig. 4, where the neighbourhood-smoothed phase maps exhibit strong suppression of pixel-wise noise and clearer recovery of the underlying structure.

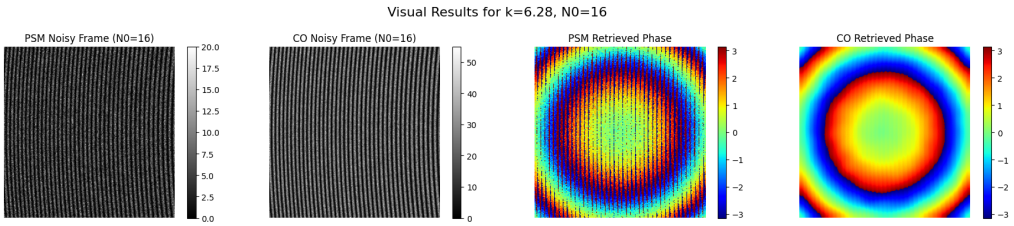

Figure 4: Comparison of phase shifting & optimisation algorithm which uses $3 * 3$ matrix neighbourhood penalty function for photon count 16 & curvature of spherical wavefront k=6.28

2.5 Phase-only Optimisation

In many holographic and interferometric imaging problems, the amplitude of the object field is either known *a priori* or is required to remain unchanged during reconstruction. To enforce this constraint, we develop a phase-only optimisation framework in which the phase of the object is iteratively updated while keeping its amplitude fixed.

Let the reference field be written as $R = |R|e^{i\phi_r}$ and the object field as $O = |O|e^{i\phi}$. Under this representation, the predicted interferometric intensity is

$$I_{\text{pred}}(\phi) = |R|^2 + |O|^2 + 2|R|\,|O|\,\cos(\phi - \phi_r). \tag{6}$$

To enforce spatial smoothness on the phase map, we employ a quadratic Total Variation penalty as shown in equation (4).

The gradient of the data-fidelity term with respect to ϕ is

$$\frac{\partial C_{\text{data}}}{\partial \phi} = 2|R|\,|O|\,(H - I_{\text{pred}}(\phi))\sin(\phi - \phi_r), \tag{7}$$

and the gradient of Ψ_{TV} is computed via Autograd's differentiation. The total gradient update is therefore

$$\nabla C(\phi) = 2|R|\,|O|\,(H - I_{\text{pred}}(\phi))\sin(\phi - \phi_r) \;+\; \alpha\,\nabla\Psi_{\text{TV}}(\phi). \tag{8}$$

Furthermore, a backtracking (Armijo) line-search strategy is used at every iteration to determine a stable step size that guarantees a sufficient decrease of the cost function. The phase estimate is then updated through

$$\phi^{(k+1)} = \phi^{(k)} - t_k\,\nabla C(\phi^{(k)}), \tag{9}$$

until convergence. This formulation ensures that only the phase is modified during the optimisation process, while the object amplitude $|O|$ remains fixed throughout.
To validate the behaviour of the phase-only optimisation in a controlled setting, we first tested the algorithm on a synthetic rectangular phase object. The ground-truth phase pattern is shown in Fig. 5(a), and a tilted plane wave was used as the reference beam (Fig. 5(b)). The corresponding interferometric intensity was generated through Eq. (6) and processed using the optimisation rule of Eq. (9). The recovered phase, shown in Fig. 5(c), closely matches the true rectangular profile and demonstrates the ability of the Total Variation penalty to enforce sharp, spatially smooth phase boundaries. This experiment confirms that the optimisation behaves correctly on simple objects before applying it to real DHM data.

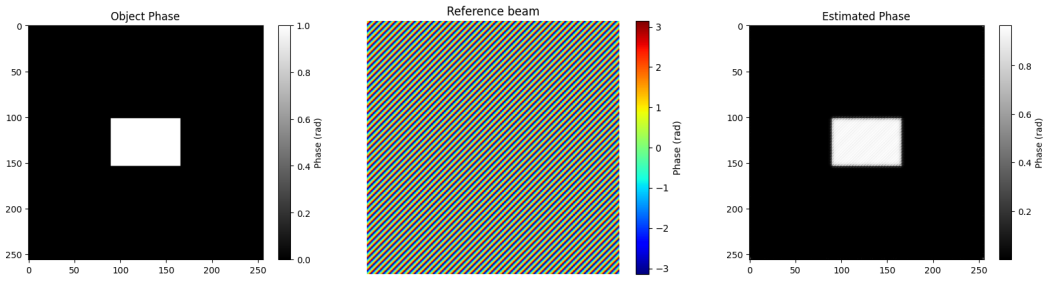

(a) (b) (c)

Figure 5: Synthetic validation of the phase-only optimisation using a rectangular phase object. Where (a) Ground-truth rectangular phase, (b) Reference beam phase, and (c) Estimated phase after optimisation

3 Phase-Only Optimisation on Real DHM Measurements

The phase optimisation pipeline was applied to a real off-axis Digital Holographic Microscopy (DHM) image of red blood cells. The experimentally recorded hologram, shown in Fig. 6(a), exhibits the characteristic high-frequency fringe pattern produced by the interference between the sample-modulated object wave and the tilted reference beam in the DHM setup. To extract the object field, the hologram was Fourier-transformed, and the resulting spectrum (Fig. 6(b)) was analysed to locate the +1 diffraction order containing the object information. A circular mask was applied around this region, which was then shifted to the centre of the spectrum and inverse-transformed to yield the reconstructed complex field $O(x, y) = |O|e^{i\phi}$. The recovered amplitude $|O|$, shown in Fig. 6(c), captures the morphological features of the RBCs, while the Fourier-derived initial phase estimate (Fig. 6(d)) provides an unregularised, noise-affected reference for subsequent optimisation.

Since the physical reference field is not measured in a single-shot DHM acquisition, an effective synthetic reference was constructed by extracting a narrow-band frequency patch around the dominant off-axis carrier in the Fourier transform of O. After re-centering and inverse-transforming this patch, we obtained an approximate reference wave $R(x, y) = |R|e^{i\phi_r}$ which is consistent with the recorded fringe structure. Using these experimentally derived object and reference fields, the predicted interferometric intensity was modelled using Eq. (6). Phase-only optimisation was then performed by keeping the object amplitude fixed and updating the phase according to the gradient expressions in Eqs. (7)–(9), together with a quadratic Total Variation prior to enforce spatial smoothness.The final optimised phase map shown in Fig. 6(e) closely resembles the ground-truth phase obtained from the +1-order reconstruction, indicating that the optimisation faithfully recovers the underlying phase structure of the RBC sample.

4 Results and discussion

Building on the work of Singh [1], we implement a constrained optimisation framework that incorporates prior knowledge about phase smoothness and spatial correlations. Unlike traditional phase-shifting methods that process pixels independently, our approach minimises a cost function that includes:
1. Data fidelity term: ensures agreement with measured interferograms
2. Regular term: Encodes expected smoothness and redundancy through total variation (TV) constraints
This method effectively models the representational correlations between neighbours,

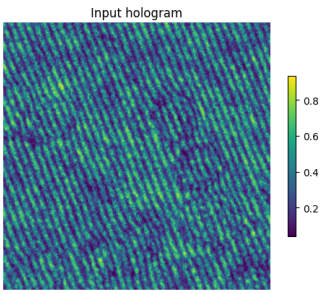

(a) Input hologram

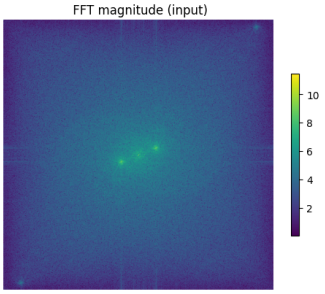

(b) Log FFT magnitude of input

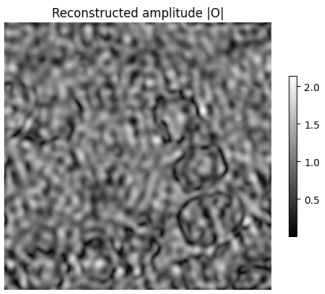

(c) Reconstructed amplitude $|O|$

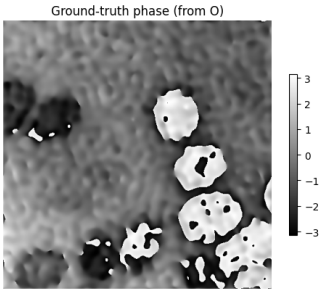

(d) Initial phase (from O)

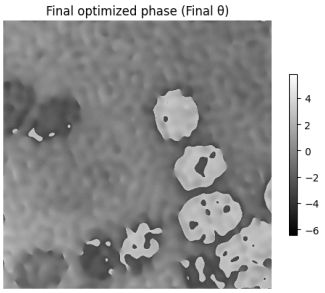

(e) Final optimised phase θ

Figure 6: Results of phase reconstruction and optimisation on the real DHM RBC image. (a) Recorded hologram; (b) Fourier magnitude showing the off-axis carrier and +1 order; (c) reconstructed object amplitude; (d) Ground truth phase; (e) final optimised phase after iterative refinement.

allowing for enhanced noise suppression and improved phase reconstruction accuracy. The behaviour of the gain G and error metrics E_{PS} and E_{CO} with respect to the photon count N_0 is shown in Fig. 7. The slopes closely match the predicted scaling, with $\log_{10}(G)$ and $\log_{10}(E_{PS})$ decreasing approximately linearly with $\log_{10}(N_0)$, while E_{CO} remains nearly constant. This behaviour is consistent with the redundancy-driven noise reduction described by Singh [1], confirming that the estimator becomes more stable as the photon budget increases.

To further validate this framework on real interferometric data, we applied the phase-only optimisation procedure to a DHM hologram of red blood cells. The +1 diffraction order was isolated from the Fourier transform of the recorded hologram to reconstruct the complex object field, while an approximate reference wave was synthesised by extracting a small, narrow-band Fourier patch and inverse-transforming it. Using these experimentally derived fields within the optimisation model, the recovered phase map closely resembled the ground-truth Fourier-based reconstruction. This demonstrates that the constrained optimisation approach generalises effectively from controlled simulations to real optical measurements, yielding stable and physically meaningful phase estimates even from a single DHM intensity image.

5 Future Scope

We plan to move beyond current limitations by incorporating more sophisticated computational techniques and expanding the scope of our analysis.

- **Advance Regularisationon & Optimization**: We will implement **Total Variation (TV) regularisation** for superior edge preservation and use **Majorization-**

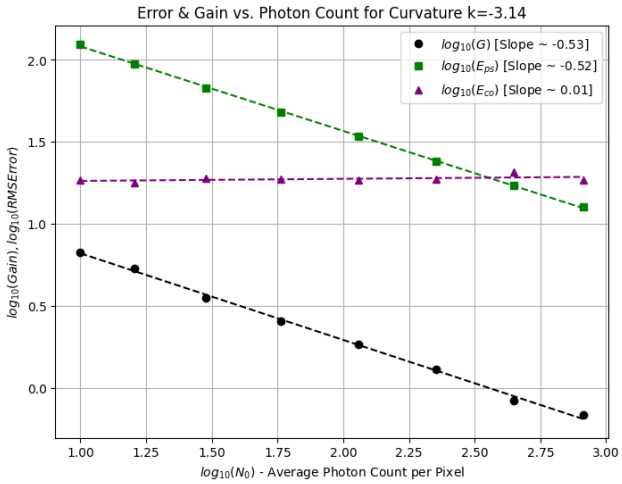

Figure 7: Reproduced plot of noise gain G, E_{PS}, and E_{CO} w.r.t. the average number of photon counts, based on the results of Singh et al.[1].

Minimization Gradient Descent (MGD) to improve convergence, supported by **adaptive parameter selection** methods.

- **Quantitative Study of Object Complexity:** A systematic, large-scale analysis across curated phase objects of increasing complexity would allow mapping phase error, redundancy gain, and photon-budget requirements onto a "complexity axis,"
- **Application to Real Biological Phase Imaging:** With additional calibration, the proposed framework can be extended to high-accuracy DHM measurements of live cells, RBC discocyte–echinocyte transitions, membrane fluctuations, and quantitative optical thickness mapping in biomedical diagnostics.
- **Hardware–Software Co-Design:** The methodology could be integrated with optimised illumination patterns, off-axis angle selection, or coded reference beams to enhance redundancy and make the optimisation more effective even at very low photon counts.

6 Conclusion

In this work, we investigated phase reconstruction under classical illumination by combining redundancy-aware modelling with constrained optimisation. Building on the principles introduced by Singh [1], we demonstrated that incorporating spatial correlations, neighbourhood structure, and Total Variation priors significantly improves phase accuracy compared to independent-pixel methods. Controlled simulations across varying photon budgets and object complexities confirmed that redundancy enables more stable and noise-resilient phase estimates. Finally, the application of our phase-only optimisation framework to a real DHM hologram of red blood cells showed that the refined phase map closely resembles the Fourier-derived ground truth while exhibiting enhanced smoothness and reduced artefacts. These results highlight the potential of optimisation-driven approaches for achieving robust quantitative phase retrieval in practical optical imaging systems.

References

[1] Singh, M., Khare, K., Jha, A. K., Prabhakar, S., & Singh, R. P. (2015). Accurate multipixel phase measurement with classical-light interferometry. Physical Review A, 91(2), 021802(R).

[2] Mandeep Singh & Kedar Khare (2018) Single-shot full resolution region-of interest (ROI) reconstruction in image plane digital holographic microscopy, Journal of Modern Optics, 65:9, 1127-1134, DOI: 10.1080/09500340.2018.1426798

[3] Emil Y Sidky and Xiaochuan Pan 2008 Phys. Med. Biol. 53 4777.

[4] Frédéric Verpillat, Fadwa Joud, Michael Atlan, and Michel Gross. Digital Holography at Shot Noise Level. JOURNAL OF DISPLAY TECHNOLOGY, VOL. 6, NO. 10, OCTOBER 2010.

[5] S.T. Thurman and J.R. Fienup. Phase-error correction in digital holography. Vol.25,No.4/April2008/J.Opt.Soc.Am.A

[6] Griesmann, U., "A Toolbox for Designing and Analysing Phase-Shifting Interferometry", National Institute of Standards and Technology (NIST) Technical Publication, 2015.

Appendix

- Jupyter notebook containing comparative analysis of phase-shifting method and constrained optimisation. Also, Establishing relationship between photon count, object complexity and error.
- Jupyter notebook containing implementation of phase-only optimisation and real data results